Chemie der Erde 75 (2015) 335–343

Contents lists available at ScienceDirect

Chemie der Erde

journal homepage: www.elsevier.de/chemer

# Hirnantian (Late Ordovician) $\delta^{13}C$ HICE excursion in a North Gondwanan (NE Spain) periglacial setting and its relationship to glacioeustatic fluctuations

Ignacio Subías[a,*], Enrique Villas[a], J. Javier Álvaro[b]

[a] Dpto Ciencias de la Tierra, Universidad de Zaragoza, 50009 Zaragoza, Spain
[b] Centro de Astrobiología (CSIC/INTA), Ctra. de Torrejón a Ajalvir km 4, 28850 Torrejón de Ardoz, Spain

ARTICLE INFO

*Article history:*
Received 1 April 2014
Received in revised form
24 November 2014
Accepted 13 May 2015
Editorial handling - P. Martinez

*Keywords:*
Chemostratigraphy
Diamictite
Unconformity
Stratigraphic gap
Glacial sequence analysis
Carbon isotopes

ABSTRACT

In the Iberian Chains of northeastern Spain, the Hirnantian Orea Shale comprises three erosive glaciogenic unconformities punctuating two transgressive glaciomarine sequences. These sequences represent ice retreat episodes of grounded ice on a North Gondwanan region of 50–60°S of estimated palaeolatitude. In contrast, the same formation recorded in the Hesperian Chains repeated episodes of extensional tectonic activity: diamictites were associated with slope-related debris flows and slumps commonly interrupted by truncating discontinuities.

An analysis of $\delta^{13}C_{org}$ in the Orea Shale has revealed that the lower Orea sequence displays isotopically light baseline values (~ −27‰) punctuated by minor (2–3‰) shifts. In distal parts, the upper sequence is characterised by a rapid rise in $\delta^{13}C_{org}$ values, which mark a positive excursion, in the range of 2.5‰ to 7‰ over 40 cm of thickness. The stratigraphic gap involved in the intra-Orea erosive unconformity appears to be greater both in proximal exposures and slope-related (Hesperian) areas, where the chemostratigraphic shift was not recorded. Upsection in the three studied sections, the $\delta^{13}C$ values display upsection a sharp return to baseline values of −26‰ to −28‰.

The Hirnantian strata of the Iberian and Hesperian Chains have recorded three major correlatable events: (i) a the karstic surface that caps upper Katian limestones and reflects the maximum glacial extension; (ii) a single $\delta^{13}C_{org}$ positive peak of ~6‰ that is recognisable in distal ramp settings, marking the beginning of the second ice retreat episode and probably representing the late Hirnantian HICE shift; and (iii) the erosive unconformity marked by the progradation of the Los Puertos shoreline complexes.



## 1. Introduction

The understanding of Late Ordovician climatic events has been greatly enhanced by the introduction of stable isotope analysis. After the relationship between Hirnantian carbon isotope excursions (HICE) and sea-level fluctuations proposed by Brenchley et al. (1994), there has been considerable discussion about the causes and patterns of the Hirnantian glaciation. Most of the early carbon isotopes analyses were conducted on carbonate strata ($\delta^{13}C_{carb}$), both on calcitic brachiopod shells and whole rock (see revisions by Brenchley et al., 2003; Melchin and Holmden, 2006). Because the Hirnantian carbonate deposits mainly developed in low palaeolatitudes, almost all of the isotopic studies were concentrated in peri-equatorial palaeocontinents, mainly in Baltica and Laurentia (e.g., Copper and Jin, 2014). The only exception is the analysis of carbon isotopes on brachiopod shells from the Argentine Precordillera, located during the Hirnantian in a periglacial setting. Nevertheless, this study analysed a single fossiliferous horizon, and although they detected heavy $\delta^{13}C$ values, the authors did not attempt to provide a complete isotopic curve.

Studies on carbon isotopes derived from the organic matter fraction ($\delta^{13}C_{org}$) have also been conducted on Hirnantian rocks (Underwood et al., 1997; Wang et al., 1997; Melchin and Holmden, 2006; Fan et al., 2009; LaPorte et al., 2009). Analysis of $\delta^{13}C_{org}$ variability was carried out in the high-palaeolatitude periglacial region of Jordan (Armstrong et al., 2005), but the black shales that were analysed form part of the final deglacial succession and do not record any of the well-known carbon isotopic shifts related to Hirnantian glacial cycles.

After the first attempts to use the Hirnantian $\delta^{13}C$ excursions as refined tools for chemostratigraphic correlation between distant areas (Brenchley et al., 1994, 2003; Marshall et al., 1997;

* Corresponding author. Tel.: +34 976 761 096; fax: +34 976 761 106.
*E-mail address:* isubias@unizar.es (I. Subías).

http://dx.doi.org/10.1016/j.chemer.2015.05.002
0009-2819/

Underwood et al., 1997), Melchin et al. (2003) suggested that the nature and trend of the $\delta^{13}C$ curves does not allow such a high-resolution because $\delta^{13}C$ curves contain both regional and global components. Only one of the two main Hirnantian positive $\delta^{13}C$ peaks from South China (Wang et al., 1997) and Arctic Canada (Melchin and Holmden, 2006) are recognised elsewhere. Thus, depending on which of the peaks is correlated with single peaks from the Baltic and Laurentian successions (Anticosti and Dob's Linn) successions, the calibration of the Hirnantian global events is different (Jones et al., 2011; Finnegan et al., 2012; Copper et al., 2013; Copper and Jin, 2014). In addition to the difficulties correlating $\delta^{13}C$ curves from incomplete successions, it must be also kept in mind that the absolute values of the $\delta^{13}C$ excursions are affected by locally acting carbon cycles (Melchin and Holmden, 2006). Nevertheless, analysis of carbon isotopes provides an opportunity for Hirnantian global correlation, as long as its limitations are recognised and the assumption is made that the Hirnantian $\delta^{13}C$ shifts are directly related to glacioeustatic sea-level changes (Finney et al., 1999; Kump et al., 1999; Villas et al., 2002; Melchin and Holmden, 2006). The potential of global isotopes analysis for global correlation is so widely acknowledged that the International Subcommission on Ordovician Stratigraphy (ISOS; Webby et al., 2004; Chen et al., 2006) has defined the boundary between the two Hirnantian stage slices (Hi1 and Hi2) to be at the end of the global Hirnantian $\delta^{13}C$ excursion HICE (Bergstrom et al., 2009). This example is the only case in which one of the Ordovician stage slices is not based on conodont or graptolite zones.

The chronostratigraphy of European Hirnantian successions from periglacial settings fringing North Gondwanaland (see Harper et al., 2013: Fig. 11.14) is still poorly constrained, which contrasts with the existing accurate chronostratigraphic information on correlative successions from North Africa (Bourahrouh et al., 2004; Villas et al., 2006; Colmenar and Álvaro, 2014). Thus, many uncertainties remain regarding the chronology of the typical Hirnantian glaciomarine strata in Europe, their stratigraphic completeness, and their relationships with the described glacial maxima and related global sea-level low-stands. According to Brenchley et al. (1991), the Hirnantian glaciomarine diamictites from the Iberian Peninsula would have been accumulated after the main glacioeustatic regression, whereas those from the Prague Basin would have pre-dated it. However, the relative sea-level fluctuations recorded in periglacial settings were also affected by isostatic depressions of the platforms caused by loading of ice sheets (Brenchley et al., 1991). A possible solution for some of these uncertainties may be the study of the carbon isotopes derived from organic matter in dark claystone diamictites or clayey sandstones from periglacial settings. An analysis of the variations in $\delta^{13}C_{org}$ values through glaciomarine strata from platforms bordering the North African margin of Gondwana could allow: (i) a chemostratigraphic correlation with the better constrained carbonate-dominated successions from low-latitude basins; (ii) a better understanding of the incompleteness of Hirnantian stratigraphic sequences represented by biostratigraphically poorly constrained diamictites interrupted by distinct glaciogenic gaps; and (iii) a comparison of chemostratigraphic shifts and ice retreat pulses. Addressing these three points would lead to a better understanding of global Hirnantian climatic events and how they may have triggered the Late Ordovician extinctions (Ghienne, 2011).

## 2. Geological setting and stratigraphy

Upper Ordovician strata are known in two areas of the Iberian Ranges in northeastern Spain: (i) the eastern Iberian Chain and (ii) several inliers that constitute its southwestern prolongation (named the Hesperian Chains), which are composed of the Aragoncillo, Nevera, Sierra Menera, and Tremedal inliers (Fig. 1). The glaciogenic character of some Upper Ordovician strata was first pointed out by Carls (1975) and Fortuin (1984). The lithostratigraphy of both areas is relatively similar and has been described by Carls (1975); Villena (1976); Hammann (1992) and Gutiérrez-Marco et al. (2002). Subsequently, Herranz Araújo et al. (2003) proposed a lithostratigraphic revision for the Hesperian Chains, where new formations were defined based on special lithic characters. We follow this updated stratigraphic sketch.

The glaciogenic shale-dominated Orea Shale Formation 50–80 m thick unconformably overlies the upper Katian Cystoid Limestone (Fig. 2). The latter is up to 50 m thick and characterised by pelmatozoan-bryozoan meadows and mud-mounds dated by means of conodonts (Carls, 1975; Sarmiento, 2002), brachiopods (Villas, 1985) and trilobites (Hammann, 1992). The shales of the Orea Formation have rarely yielded unreworked organic-walled microfossils. Although acritarchs reported from the lower part of the Orea Formation were dated by Hafenrichter (1979) as Silurian, Vecoli (pers. comm.) suggests that the association is not distinctive enough to discriminate between Ordovician and Silurian strata. More recently, Vizcaïno et al. (2004) described the presence of the only biostratigraphically significant fossils of the Orea Formation. They reported the occurrence of *Mucronaspis mucronata*, a biogeographically widespread Hirnantian trilobite commonly associated with the Hirnantia Fauna (Owen et al., 1991), close to Noguera (Tremedal inlier). *M. mucronata* occurs in the Noguera section (reported below as section NOR), 2 m above the base of the Orea Formation. Although its presence confirms the Hirnantian age of the unit, it is not stratigraphically precise enough to discriminate between the two graptolite zones or the two stage slices of the Hirnantian Stage (Bergstrom et al., 2009).

In the eastern Iberian Chain, the Orea Formation contains two distinct transgressive depositional sequences (related to the retreat of grounded ice). These sequences are underlain by two pronounced glaciogenic discontinuities (D1 and D2 in Fig. 2; for a detailed description of facies associations and sequence framework, see Álvaro and Van Vliet-Lanoë, 2009). The lower sequence consists of offshore-dominated shales recorded in proximal outcrops passing basinward into sedimentation of mixed massive diamictites, rich in carbonate dropstones. These are associated with intraformational slumps and local synsedimentary bedding distortion at the Valdelaparra section (VP). The limited extent of the associated carbonate dropstone-bearing wedge and the record of unstable substrates may reflect the underflow action of active glacier fronts. The diamictites of the lower sequence formed extensive blanket-like sheets that draped over pre-existing karstic palaeotopographies (D1). In proximal outcrops, the upper sequence of the Orea Formation is absent due to erosion, and D2 directly coincides with the erosive base of the overlying Los Puertos Formation (D3). In central sections (shoreward of the Valdelaparra section, VP, and Peña del Tormo section, PT), D2 is represented by an abrupt change from open-sea offshore sediments, which lack distinct records of glaciogenic processes (lower sequence), to conglomeratic channels covered by terrigenous glaciomarine diamictites (upper sequence), indicating abrupt changes in depositional conditions. The upper sequence consists of massive homogeneous, terrigenous diamictites, considered to be the result of floating, debris-bearing ice. The ice was probably in the form of a discontinuous ice platform or a series of ice platforms that deposited glaciomarine dropstones in areas of high sedimentation rates with little current reworking. D2 is marked by conglomeratic channels that change into calcareous sandstones (rich in limestone and dolostone granules) and limonitised bioclasts (dominated by disarticulated and broken echinoderm and bryozoan debris).

In contrast, the beginning of the Hirnantian in the Hesperian Chains recorded an episode of extensional tectonics, characterised

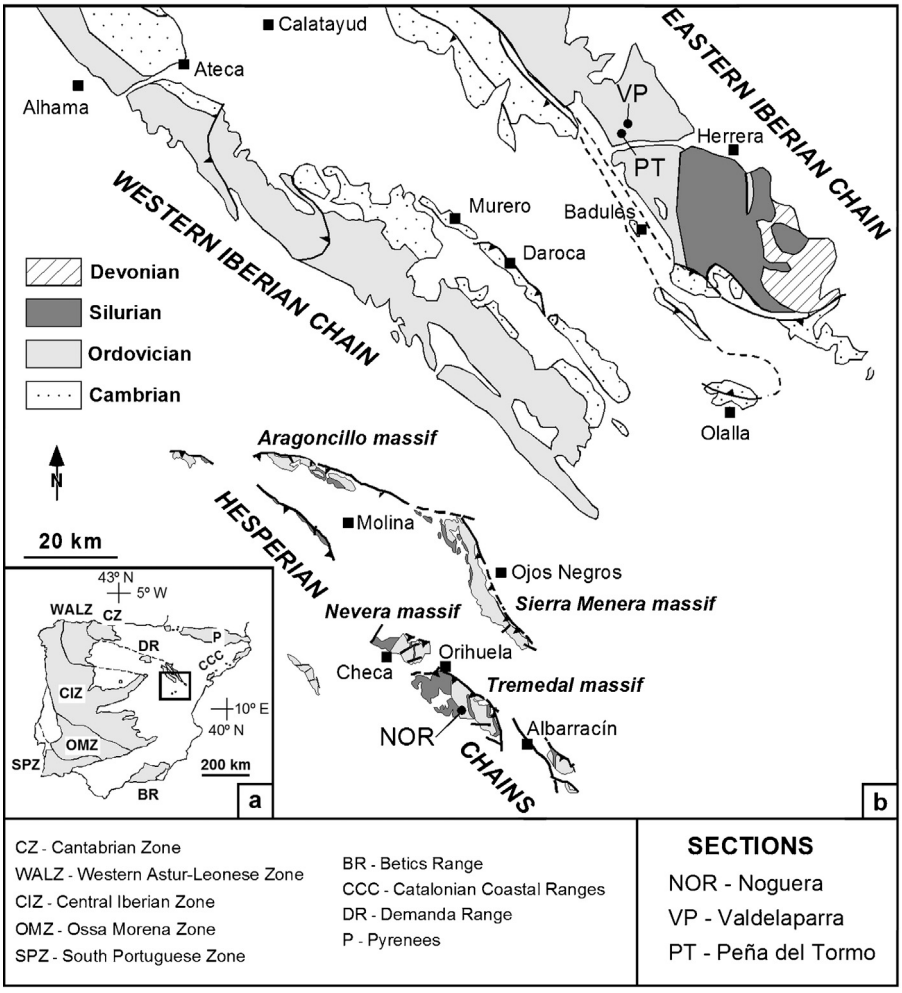


**Fig. 1.** Generalised map of the Palaeozoic in both Iberian Chains and Hesperian Chains with position of sampled locations; modified from Álvaro and Van Vliet-Lanoë (2009).

by a series of NW–SE trending drowning palaeohighs and grabens with encased hydrothermal Fe ore deposits (Fernández-Nieto et al., 2003; Álvaro and Van Vliet-Lanoë, 2009). Most of the Orea diamictites close to palaeohighs were associated with debris flows generated by slumping, which is evidence of resedimentation and "cannibalistic" processes on upper slopes. Tectonic movements coeval with the Orea deposition are also suggested by thickness variations of facies associations and the common occurrence of chaotic and contorted bedding. Abrupt vertical and lateral variations are associated with overlying synsedimentary slumped beds, local erosive discontinuities, sedimentary slides, debris flows, associated olistolithic beds and breccia sheets. This suggests the local breakdown and instability of the seafloor, the development of active depositional slopes, and the lack of the distinct sequences described in the eastern Iberian Chain (Álvaro and Van Vliet-Lanoë, 2009).

The overlying Los Puertos Formation is 1–50 m thick and consists of white sandstones and conglomerates with rare shale intercalations. The formation is underlain by another major erosive unconformity (D3 in Fig. 2). The formation has been currently considered to represent the basal Silurian, based on its Rhuddanian to Aeronian graptolites occurring in clayey intercalations (Gutiérrez-Marco and Štorch, 1998). Nevertheless, the occurrence of a low diversity Hirnantia Fauna in the lower horizons of the Criadero Quartzite (Villas et al., 1999), and in the Luna Quartzite (Gutiérrez-Marco et al., 2010a,b), a lateral equivalent of the Los Puertos Formation in Central and North Spain, respectively, suggests that the Ordovician-Silurian boundary may be tentatively placed within the Iberian unit. The recent discovery of a Hirnantia Fauna within the Los Puertos Formation itself (Bernárdez et al., 2014) confirms the correlation above.

## 3. Methods

We selected three reference sections for chemostratigraphic analysis: (i) the palaeogeographically proximal Valdelaparra ravine (VP) section of the eastern Iberian Chain (representing a quiescent, intra-platform ramp); (ii) the distal Peña del Tormo hill (PT) section of the eastern Iberian; (iii) and the Noguera locality (NOR), which is a section of the Tremedal inlier in the Hesperian Chains representative of a tectonically active outer-shelf (Fig. 1). We analysed 23 and 17 diamictite samples from the two reported sequences of the Orea Formation in the VP and PT sections. The VP and PT sampled sections have a thickness of 24 and 22 m, respectively. We analysed 32 samples of grey to black shale spanning a monotonous blackish shale succession, 103 m thickness in Noguera.

After grinding and homogenising the selected samples to <53 μm, their bulk mineralogy was studied by X-ray diffractometry (XRD). Oriented aggregates (OA) were prepared by both the <2 μm and <20 μm fractions. The aggregates were separated by sedimentation. The oriented aggregates were chemically treated by saturation with ethylene glycol and dimethyl sulfoxide. Semi-quantitative estimates were conducted using the main peak of every phase, according to Schultz (1964) and Biscaye (1965)

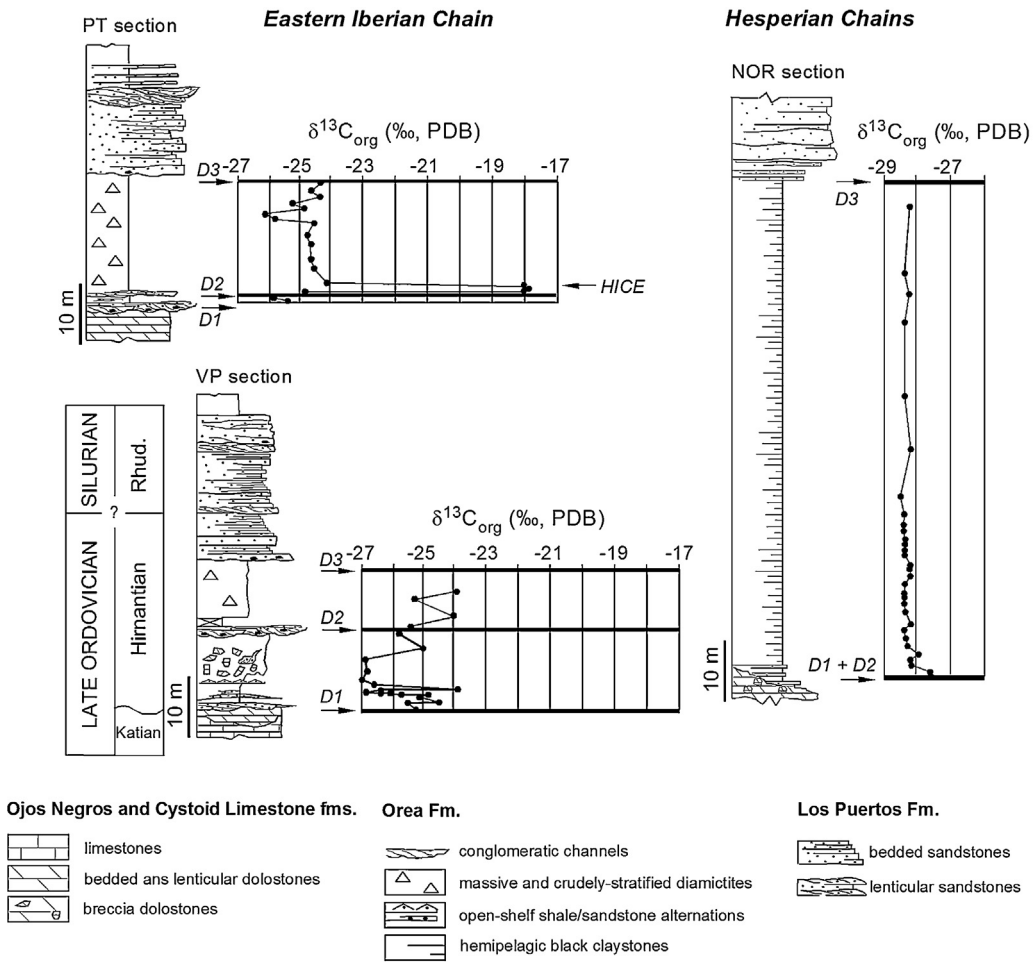


**Fig. 2.** Stratigraphic logs and $\delta^{13}C_{org}$ curves at Valdelaparra (VP), Peña del Tormo (PT) and Noguera (NOR) sections; modified from Álvaro and Van Vliet-Lanoë (2009). Figures on the right side of the columns correspond to analysed samples.

intensity factors. The samples were analysed using a Philips PW 1710 diffractometer set at Cu*K*α radiation with an automatic slit and a diffracted-beam graphite monochromator.

We follow the Larson et al.'s (2008) in situ method to process the studied samples. This method was originally designed for the removal of siderite. We made this choice due to the rare presence of calcite in samples and to avoid the loss of soluble organic material during acidification.

Powdered samples were placed in silver capsules and weighed. Sample capsules were left open and placed on a plastic sample tray for acidification. Each day, 100 ml of 6 N HCl was pipetted into the open sample capsules and allowed to evaporate overnight. This volume of acid was chosen so that all of the solid sample and aqueous components would remain within the capsules. Acid was added at the beginning of each day of pre-treatment. The samples were never rinsed, and acid was not decanted during acidification. Following pre-treatment, samples were dried in an oven at 50 °C, removed and weighed. Sample capsules were then tightly closed for isotopic and elemental analysis. The samples were put in a rotating carrousel for combustion in a HCNOS Eurovector EA 3000 elemental analyser. The gas sample was subsequently purified and passed through an ISOPRIME continuous flow dual-inlet mass-spectrometer for elemental and isotopic analysis. Total organic carbon content was estimated from $CO_2$ yields prior to isotope analyses. Carbon isotope ratios were measured against international and internal standards. The results are expressed in the notation δ (‰) in relation to PDB scale. Analytical reproducibility of replicate samples using this method was better than 0.1‰.

## 4. Results and discussion

As stated above, systematic mineralogical and organic carbon isotopic chemostratigraphy was carried out for the Orea Formation along two sections in the eastern Iberian Range, Valdelaparra ravine (VP) and Piedra del Tormo hill (PT), and one section in the Hesperian Chains, Noguera (NOR) (Fig. 1—full results are displayed in Tables 1 and 2).

### 4.1. Mineralogical tracers: dealing with diagenesis

Generally speaking, knowledge of the phyllosilicate assemblage and its crystallochemical parameters allow post-depositional evolution to be monitored. For Ordovician terrigenous sedimentary rocks of the Iberian Chains, Bauluz et al. (1998) proposed an evolutionary trend from diagenesis to low-grade anchizone. Our mineralogical study was designed to address the extent to which diagenesis may alter the original isotopic ratios recorded by the studied diamictites and claystones and to evaluate its influence on further palaeoceanographic interpretations.

The mineralogical assemblages mainly comprise quartz, mica, chlorite and subsidiary feldspar (Table 1). Occasionally, calcite was detected as a rare component in the PT and VP sections, and it was eliminated before analysis by the procedure described above. In

**Table 1**
Mineralogical composition (XRD) of whole rock and <20 mm and <2 mm fractions of the studied samples. Illite crystallinite (IC) values of <2 mm fraction are also included.

| | Whole rock | | | | <20 μm Fraction | | | <2 μm Fraction | | | |
|---|---|---|---|---|---|---|---|---|---|---|---|
| Section | Q | Fdp | Phy | Cte | I | Ka | Chl | I | Ka | Chl | IC |
| **VP** | 36–60 | 3–9 | 34–59 | 0–3 | 88–96 | 0–5 | 4–7 | 83–92 | 0–6 | 4–11 | 0.31–0.50 |
| *n* = 16 | 49 | 4 | 46 | 1 | 91 | 3 | 6 | 90 | 2 | 8 | 0.45 |
| **PT** | 38–62 | 0–4 | 37–50 | 0–6 | 89–100 | 0–5 | 0–7 | 85–100 | 0–8 | 3–7 | 0.49–0.79 |
| *n* = 17 | 51 | 2 | 45 | 2 | 94 | 2 | 4 | 94 | 2 | 4 | 0.71 |
| **NOR** | 37–52 | 4–9 | 39–61 | – | 39–90 | 0–15 | 3–60 | 57–94 | 0–18 | 1–45 | 0.29–0.61 |
| *n* = 32 | 44 | 5 | 51 | – | 57 | 3 | 40 | 68 | 3 | 29 | 0.43 |

fine fractions, the main phases were illite and chlorite, with small amounts of kaolinite (Table 1). The illite crystallinity (IC) values ranged from 0.31 to 0.50°2$\theta$, from 0.49 to 0.79°2$\theta$, and from 0.29 to 0.61°2$\theta$ for the VP, PT, and NOR sections, respectively (Table 1). These values are indicative of a diagenetic to anchizone grade. No trend of significant variability was observed at the local or regional scales of the studied sections in silt or clay fractions.

### 4.2. X-ray diffraction profiles

The bulk mineralogy, determined by XRD, mainly comprises quartz, phyllosilicates (mica and chlorite) and scarce feldspars, which displayed an upsection replacement of kaolinite (reworked from karstic infills associated with the underlying D1 discontinuity) by feldspar at the lowermost part of the sequences. Few samples from the VP and PT sections contain calcite as accessory mineral, probably also related to the reworking of scattered carbonate clasts and fossils from the underlying Cystoid Limestone. Dioctahedral mica was the main constituent of the <20 and <2 μm fractions. Whereas significant amounts of chlorite were detected in all samples, kaolinite was only found at the bottom of the studied sections.

The IC (CIS) values of the <2 μm oriented aggregates were in the range of 0.29 to 0.89. This variation is irrespective of the stratigraphic position. Value fluctuations were not gradual; there were some abrupt changes, probably related to the presence of scattered dropstones. The aforementioned values correspond to diagenesis and anchizone-grade metamorphism. The above data are compatible with those obtained by Bauluz et al. (1998) in Cambrian-Ordovician shales and greywackes from the central Iberian Chains.

### 4.3. Isotope profiles

Plotting $\delta^{13}C_{org}$ versus stratigraphic height for PT, VP, and NOR sections (Fig. 2) revealed that the chemostratigraphic transect is distinctly constrained by the setting and timespan involved in the erosive unconformity that separates the aforementioned lower and upper sequences (D2). The lower sequence was characterised by isotopically light baseline values (∼ −27‰) punctuated by minor (<2−3‰) shifts. In the distal palaeogeographic area of the Iberian ramp (PT), the upper sequence was characterised by a rapid rise in $\delta^{13}C_{org}$ values that mark a positive excursion, on the order of 2.5‰ to 7‰ over 40 cm of thickness. This sample was situated over 2.2 m at the base of D2. Although the isotopic excursion is represented by a thin stratigraphic interval, this anomaly is robust because the analysis was reproduced three times through the particular, calcite-free stratigraphic interval. In contrast, the stratigraphic gap involved in the unconformity D2 would be expected to be greater both in proximal exposures (such as VP) and tectonically active areas (NOR), where the onset of marine conditions was delayed. The $\delta^{13}C_{org}$ values were higher in the three studied sections, and they displayed a sharp return to the baseline values, ranging from −27‰ in the Iberian ramp to −28‰ in the Hesperian shelf. Finally, $\delta^{13}C_{org}$ values remained invariant at the NOR section, whereas an abrupt decline above the positive shift was observed at the PT and VP sections. Therefore, the described differences in the shape of the profiles (Fig. 2) are linked to palaeogeographic differences, specifically proximal intra-shelf ramp versus outer shelf settings. It is important to remember that the NOR section is marked by the presence of trilobite-bearing black claystones, and the PT and VP sections consist of light-coloured siltstones bearing burrowing traces; thus, there is no evidence of anoxic conditions for the latter sections.

Based on the clay composition of the studied sections and those reported at the regional scale (Bauluz et al., 1998), we concluded that the largest post-depositional influence recorded by the rocks was related to burial diagenesis. Furthermore, we determined that the studied sections experienced a similar diagenetic trend. Therefore, we suggest that the major changes in isotopic values reflect primary changes. This suggestion is also supported by the fact that the PT section recorded a carbon isotope excursion that mimics a similar shift found in subtropical Hirnantian platforms (Brenchley et al., 2003 and references therein; Finnegan et al., 2012, Jones et al., 2011). Absolute values must be regarded with caution, but there is no evidence for a diagenetic alteration sufficient to greatly change the original $\delta^{13}C$ trends. This is in agreement with Schwab et al. (2005), who stated that carbon isotope signals show little or no evidence of alteration under anchizone-grade metamorphism conditions.

As the diagenetic alteration is of particular concern when constructing an isotopic profile, it is necessary to consider the effects of diagenesis on primary $\delta^{13}C_{org}$ values. This must be accomplished by taking into account the low total organic carbon (TOC) concentrations in the studied samples: from 0.15 to 0.44% in the VP section, 0.19 to 0.32% in the PT section, and 0.37 to 0.65 in the NOR section. Data collected by Bauluz et al. (1998) and this study have shown that all Ordovician sediments have undergone diagenetic modification that promoted organic matter alteration, showing an evolutionary trend towards isotopically heavier values. By comparing our data with those compiled by Melchin et al. (2003) and Melchin and Holmden (2006), $\delta^{13}C_{org}$ values from localities showing no alteration (e.g., Arctic Canada and Dob's Linn, Scotland) are relatively lighter (baseline between −32 and −30‰), but they are generally only in the Katian and uppermost Hirnantian strata, which were not sampled/available in this study. Therefore, absolute values must be regarded with caution. The presence of a positive $\delta^{13}C_{org}$ shift over the same stratigraphic interval in a palaeogeographically distal ramp section suggests that there is no diagenetic alteration gradient throughout the studied sections and that the $\delta^{13}C_{org}$ positive excursion in the Iberian ramp correlates with that reported worldwide through the Hirnantian. These findings indicate that the isotopic data are recording changes at a global scale.

## 5. Comparison with chemostratigraphic and global sea-level curves

Melchin and Holmden's (2006) results from Arctic Canada depict two main $\delta^{13}C$ positive excursions throughout the Hirnantian.

**Table 2**
$\delta^{13}C_{org}$ composition of the sampled sections.

| Sample | Height (m) | $\delta^{13}C_{PDB}$ (‰) |
|---|---|---|
| **VP section** | | |
| VP-21 | 21.7 | −23.9 |
| VP-20 | 19.9 | −25.3 |
| VP-19 | 17.7 | −24.0 |
| VP-18 | 15.7 | −25.4 |
| VP-17 | 13.5 | −25.8 |
| VP-16 | 11.7 | −24.0 |
| VP-15 | 8.5 | −26.9 |
| VP-14 | 5.9 | −26.8 |
| VP-13 | 4.4 | −27.0 |
| VP-12 | 3.4 | −26.6 |
| VP-11 | 2.4 | −23.8 |
| VP-10 | 2.2 | −26.3 |
| VP-9 | 2.1 | −26.9 |
| VP-8 | 2.0 | −26.3 |
| VP-7 | 1.9 | −26.1 |
| VP-6 | 1.8 | −25.8 |
| VP-5 | 1.7 | −24.8 |
| VP-4 | 0.9 | −25.1 |
| VP-3 | 0.8 | −24.5 |
| VP-2 | 0.5 | −25.5 |
| VP-1 | −0.5 | −25.3 |
| **PT section** | | |
| PT-17 | 22.4 | −24.3 |
| PT-16 | 20.8 | −24.6 |
| PT-15 | 19.5 | −24.3 |
| PT-14 | 18.2 | −25.3 |
| PT-13 | 16.9 | −24.8 |
| PT-12 | 16.0 | −26.2 |
| PT-11 | 15.0 | −25.8 |
| PT-10 | 14.0 | −24.5 |
| PT-9 | 12.0 | −24.7 |
| PT-8 | 10.5 | −24.6 |
| PT-7 | 8.0 | −24.6 |
| PT-6 | 6.5 | −24.5 |
| PT-5 | 4.0 | −24.9 |
| PT-4 | 3.2 | −24.1 |
| PT-3b | 2.3 | −18.0 |
| PT-3 | 2.2 | −17.9 |
| PT-3a | 2.1 | −18.1 |
| PT-2 | 0.3 | −24.8 |
| PT-1 | 0.2 | −25.4 |
| **NOR section** | | |
| NOR-51 | 94.5 | −27.3 |
| NOR-48 | 83.5 | −26.9 |
| NOR-46 | 80.1 | −27.4 |
| NOR-44 | 75.5 | −27.9 |
| NOR-38 | 63.4 | −28.0 |
| NOR-32 | 54.6 | −27.3 |
| NOR-27 | 46.7 | −27.9 |
| NOR-26 | 45.3 | −27.6 |
| NOR-25 | 43.6 | −27.7 |
| NOR-24 | 41.4 | −27.9 |
| NOR-23 | 40.3 | −27.8 |
| NOR-22 | 38.8 | −27.7 |
| NOR-21 | 37.9 | −27.7 |
| NOR-20 | 36.9 | −27.7 |
| NOR-19 | 35.9 | −27.6 |
| NOR-18 | 34.1 | −27.2 |
| NOR-17 | 33.5 | −27.3 |
| NOR-16 | 32.3 | −27.2 |
| NOR-15 | 30.9 | −27.4 |
| NOR-14 | 29.3 | −27.5 |
| NOR-13 | 28.5 | −27.5 |
| NOR-12 | 27.4 | −27.7 |
| NOR-11 | 25.8 | −27.5 |
| NOR-10 | 23.7 | −27.2 |
| NOR-9 | 22.7 | −27.7 |
| NOR-8 | 19.7 | −27.5 |
| NOR-7 | 18.1 | −27.4 |
| NOR-5 | 17.2 | −26.8 |
| NOR-4 | 17.2 | −27.1 |
| NOR-3 | 16.3 | −27.2 |
| NOR-2 | 15.0 | −26.4 |
| NOR-1 | 14.1 | −26.3 |

These excursions are at similar stratigraphic positions than those of the isotopic curve from South China (Wang et al., 1997). The results from both regions show that a positive $\delta^{13}C_{org}$ excursion of 3–6‰ (Fig. 3) begins just below the base of the Hirnantian, peaking in the lower part of the *Normalograptus extraordinarius* Zone (early Hirnantian). A second peak of similar magnitude occurs in the lower part of the *N. persculptus* Zone (late Hirnantian; Melchin and Holmden op. cit.). Although the timing of peak positive excursions is not completely isochronous between different regions (Melchin and Holmden, 2006; Delabroye and Vecoli, 2010), the early Hirnantian peak appears to be suppressed or incompletely recorded outside South China and Laurentia (see also Jones et al., 2011, Finnegan et al., 2012). Both in South China and Laurentia (Wang et al., 1997; Melchin and Holmden, 2006; LaPorte et al., 2009), the late-Hirnantian $\delta^{13}C_{org}$ excursion of $2.7 \pm 0.4$‰ (significantly smaller than the 5–7‰ positive shifts recorded in epeiric, carbonate-dominated platform settings) is correlatable with a negative shift in wt. % TOC contents of ~4%. The single positive peak in the $\delta^{13}C$ curves from the Baltic region is confidently correlated with the upper peak in Arctic Canada and South China (Melchin and Holmden, 2006). As pointed out by Melchin and Holmden (op. cit.), the two prominent peaks in the $\delta^{13}C_{org}$ identified in South China and Arctic Canada seem to have been triggered by two eustatic falls related to major glacial pulses identified in West Africa (Ghienne, 2003, 2011; Loi et al., 2010), Turkey (Monod et al., 2003), and North Africa (Le Heron et al., 2006).

In the Iberian Ranges, the Hirnantian strata overlie a glaciogenic karstic surface (D1) that marks the top of upper Katian limestones (Carls, 1975; Hafenrichter, 1979; Vennin et al., 1998; Álvaro and Gutiérrez-Marco, 2007). The diamictites sandwiched between D1 and the erosive unconformity that separates the two Orea sequences (D2) show an irregular $\delta^{13}C_{org}$ pattern in VP and PT, which cannot be correlated with the aforementioned early Hirnantian positive $\delta^{13}C_{org}$ shift. Above D2, the single positive peak in $\delta^{13}C_{org}$ of ~6‰, identified in the distal (palaeogeographic) exposures of the upper Orea sequence, probably corresponds to the worldwide positive excursion, considered to be late Hirnantian in age (lower part of the *persculptus* Zone; Melchin and Holmden, 2006). The $\delta^{13}C_{org}$ gradient of 2.5 to 7‰ recorded in PT (Fig. 3) mimics the maximum values reported in epeiric seas, a factor probably controlled by the palaeogeographic setting of the Iberian section. The reduced thickness (40 cm) involved in the HICE shift in PT must be interpreted in terms of a dramatically reduced availability of accommodation space.

The lower Hirnantian (*extraordinarius* Zone) strata in the Hesperian shelf would be absent due to the amalgamation of D1 and D2 (Álvaro and Van Vliet-Lanoë, 2009). In the Iberian ramp, the record of the lower Hirnantian would be constrained by the diachronous gaps involved in D1 and D2. D1 would correspond to the initial glacial episodes that led to the emersion of North Gondwana and the karstification of its Katian limestones. The subsequent flooding of the Iberian ramp was interrupted by a regression, which is represented by the glaciogenic unconformity D2. The coincidence of this regression with the peak of the HICE shift is documented by its presence in distal parts of the Iberian intra-platform ramp (PT) overlying D2. The retrogradation of these glaciogenic coarse-grained siliciclastic deposits (associated with D2) should have led to shale deposition earlier in the proximal parts of the Iberian ramp (VP) than in the slope-related environments of the Hesperian shelf, where the peak of the HICE was not recorded. Although this second major glacial pulse is considered to have caused the maximum glacial advance and the greatest global eustatic fall (Ghienne, 2003, 2011; Monod et al., 2003; Le Heron et al., 2006), the Iberian ramp only underwent a brief emersion and should have been able to record the late Hirnantian $\delta^{13}C_{org}$ positive excursion in its most distal parts. This second erosive unconformity

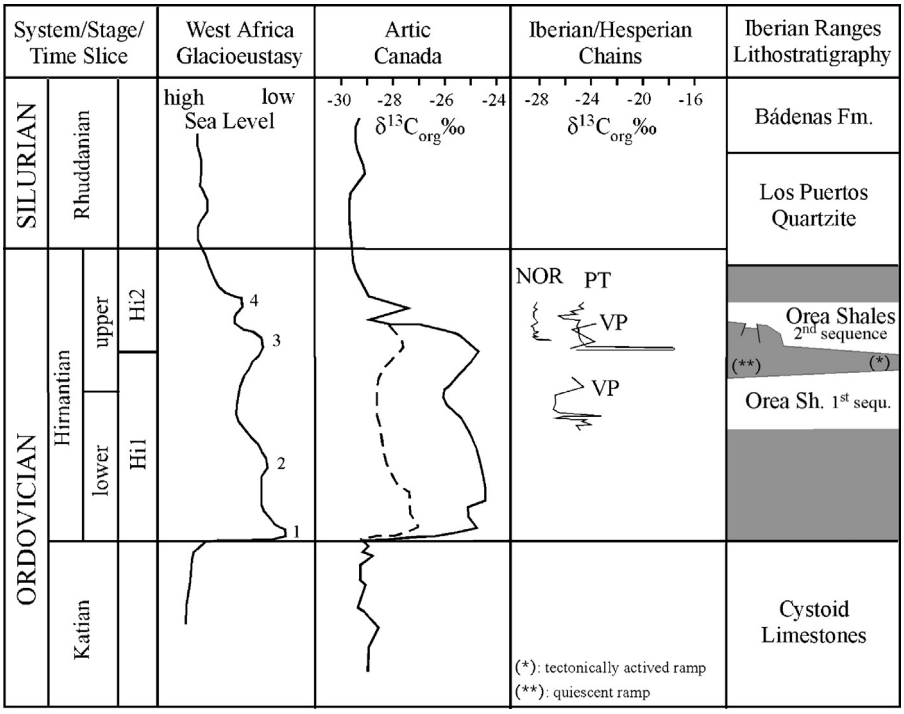


**Fig. 3.** Tentative correlation of the organic carbon isotope curve from the studied sections in the Iberian Chains and Hesperian Chains, with the composite organic carbon isotope curve from Artic Canada (Melchin and Holmden, 2006), the glacioeustatic sea-level curve proposed by Ghienne (2003), and the proposed correlation by Melchin and Holmden (2006: Fig. 7). Numbers on the sea-level curve represent the four high-frequency glacial cycles recognised by Ghienne (2003) in Mauritania (West Africa).

(D2) affected successions variably throughout the Iberian ramp by modifying the thickness of the second Orea sequence in proximal-distal transects. The early drowning of the Iberian ramp reinforces the suggestion of an isostatic depression caused by the loading of a growing or advancing ice sheet (Brenchley et al., 1991). Palaeovalleys related to the Hirnantian glacial event were described in northern Spain by Gutiérrez-Marco et al. (2010a,b) who suggested they were related to the Hirnantian North Gondwana ice sheet that would have reached the Ibero-Armorican domain. The same relation with the North Gondwana ice sheet can be presumed for the ice mass responsible of the isostatic depression and drowning of the Iberian ramp. The size and loading effect of the ice sheet would have been enough to submerge the region during this second and most important glacial pulse.

The Los Puertos Formation is the local representative in the Iberian Ranges of the widespread quartzitic unit that overlies the Hirnantian diamictites in most of Iberia and the Pyrenees. It could also be correlated with the Upper Second Bani Formation in the Moroccan Anti-Atlas. The Iberian quartzitic units capping the Hirnantian glacial succession have been interpreted to result from isostatic rebound after the melting of the Hirnantian ice cap (Villas et al., 2002; Gil-Peña et al., 2004; Álvaro and Van Vliet-Lanoë, 2009). However, in some Gondwana margins, the isostatic rebound could almost have been compensated by Gondwanan ice-sheet melting.

The two higher frequency cycles within each of the two major glacial cycles related to the C isotopic peaks that have been recognised in Mauritania (Ghienne, 2003) and Turkey (Monod et al., 2003) could provide a more suitable interpretation of the deposition of the Los Puertos Formation. This sandstone unit may be related to the fourth and last of those high-frequency glacial cycles. The fourth is considered the least intense of the four cycles and marks the definitive flooding of the cratonic platforms after final melting of the Gondwanan ice cap (Ghienne, 2003, 2011; see also glacial interpretations of Desrochers et al., 2010).

In summary, the Hirnantian record of the Iberian ramp and the Hesperian shelf shows three major regressions (responsible for the onset of three erosive unconformities: D1 to D3) separating two glaciogenic flooding sequences. D2 is nearly synchronous with the record of the HICE shift, associated with subglacial erosion and globally related to the late-Hirnantian glacial climax (Ghienne, 2003, 2011; Loi et al., 2010). As stated by Melchin and Holmden (2006), these data support the hypothesis that the $\delta^{13}C$ shifts seem to be the result of increased rates of weathering of carbonate platforms that were exposed during the glacioeustatic sea-level falls.

## 6. Conclusions

In the Iberian and Hesperian Chains of NE Spain, the contact between the Katian Cystoid Limestone and the glaciomarine Orea Formation is marked by a karstic unconformity. In the Iberian ramp, the Hirnantian Orea Shale Formation comprise two transgressive sequences that represent the retreat of grounded ice: (i) proximal offshore shales passing basinward into sedimentation of massive, mixed diamictites rich in carbonate dropstones and (ii) homogeneous, terrigenous massive diamictites. Both sequences are separated by an erosive unconformity characterised by conglomeratic channels, which wedge out distally and change into calcareous sandstones rich in limestone and dolostone granules. By contrast, the Hesperian shelf recorded an extensional tectonic activity that led to a different sequence arrangement of the Orea Formation. Close to the palaeohighs, the diamictites were associated with debris flows generated by slumping evidence of resedimentation and "cannibalistic" processes on upper slopes.

An analysis of $\delta^{13}C_{org}$ in the Orea Shales revealed differences related to their palaeogeographic setting. Although each chemostratigraphic transect is distinctly constrained by the setting and timespan involved in the erosive unconformity that separates the two Orea sequences, the lower sequence was characterised by isotopically light baseline values (~ −27‰) punctuated by minor (<2–3‰) shifts. In distal parts of the Iberian ramp, the upper

sequence was marked by a rapid rise in $\delta^{13}C_{org}$ values that mark a positive excursion, ranging from 2.5‰ to 7‰. In contrast, the stratigraphic gap involved in the erosive unconformity that separates both Orea sequences was greater both in proximal exposures of the Iberian ramp and slope-related areas (Hesperian shelf), where the onset of marine conditions was delayed and the chemostratigraphic shift was not recorded. The $\delta^{13}C$ values were higher in the three studied sections and display a sharp return to the baseline values of −26‰ to −28‰.

As a result, the Hirnantian strata recorded in northeastern Spain record three major correlatable events: (i) the karstic surface that caps the upper Katian limestones, which reflects the maximum glacial extension in the study area; (ii) a single positive peak in $\delta^{13}C_{org}$ of 6‰, exclusively recognisable in distal ramp exposures of the upper Orea sequence (directly overlying a major erosive unconformity), which probably corresponds to worldwide late-Hirnantian (lower part of the *persculptus* Zone) positive excursion; and (iii) the erosive unconformity marked by the progradation of the coastal and shoal complexes represented by the Los Puertos Quartzite.

Therefore, lower Hirnantian (*extraordinarius* Zone) strata appear to be absent in the Hesperian shelf and incompletely represented in the Iberian ramp. Their lower part would be constrained by the initial glacial episodes that led to the emersion of North Gondwana and the karstification of its exposed Katian carbonate platforms, and their upper part would be constrained by the stratigraphic gap involved in the unconformity that separates both Orea sequences. The early Hirnantian flooding of the Iberian ramp pre-dated the second major pulse of the late Hirnantian glaciation, marked in the study area by an erosive unconformity and the HICE $\delta^{13}C_{org}$ positive excursion. Although this second major glacial pulse is globally considered to have caused the maximum glacial advance and the greatest eustatic fall, the Iberian ramp only underwent a brief emersion in its most distal parts.

## Acknowledgements

The authors thank reviewers' suggestions, which have contributed to a better understanding of the ideas expressed in a previous version. This is a contribution to Projects CGL2009–09583, CGL2012-39471 and CGL2013–48877of Spanish MINECO and EU-FEDER. It is also a contribution to the IGCP 591 project "The Early to Middle Paleozoic Revolution".

## References

Álvaro, J.J., Gutiérrez-Marco, J.C., 2007. Field trip to the Ordovician–Silurian transition of the Palaeozoic inliers in the Teruel and Guadalajara provinces, Spain. In: IGCP-503 Regional Meeting and Field-trip. Zaragoza University Press, Zaragoza, pp. 38–43.

Álvaro, J.J., Van Vliet-Lanoë, B., 2009. Late Ordovician carbonate productivity and glaciomarine record under quiescent and active extensional tectonics in NE Spain. In: Bassett, M.G. (Ed.), Early Palaeozoic Peri-Gondwana Terranes: New Insights from Tectonics and Biogeography. Geological Society, London, pp. 117–139, Special Publications 325.

Armstrong, H.A., Turner, B.R., Makhalouf, I.M., Weedon, G.P., Williams, M., Smadi, A.A., Salah, A.A., 2005. Origin, sequence stratigraphy and depositional environment of an Upper Ordovician (Hirnantian) deglacial black shale, Jordan. Palaeogeogr. Palaeoclimatol. Palaeoecol. 220, 273–289.

Bernárdez, E., Colmenar, J., Gutierrez-Marco, J.C., Zamora, S., 2014. New peri-Gondwanan records of the Hirnantia Fauna in the latest Ordovician of Spain. In: Pankhurst, R.J., Castiñeiras, P., Sánchez Martínez, S. (Eds.), Gondwana 15, North meets South. 15, Abstracts Book, International Association for Gondwana Research IGCP Projects 574, 591, 596, 597 & 628 (IUGS-UNESCO).

Bauluz, B., Fernández-Nieto, C., González López, J.M., 1998. Diagenesis-very low-grade metamorphism of clastic Cambrian and Ordovician sedimentary rocks in the Iberian Range (Spain). Clay Miner. 33, 373–393.

Bergstrom, S.M., Chen, X., Gutiérrez-Marco, J.C., Dronov, A., 2009. The new chronostratigraphic classification of the Ordovician System and its relations to major regional series and stages and to $\delta^{13}C$ chemostratigraphy. Lethaia 42, 97–107.

Biscaye, P.E., 1965. Mineralogy and sedimentation of recent deep-sea clay in the Atlantic ocean and adjacent seas and ocean. Geol. Soc. Am. Bull. 76, 803–832.

Bourahrouh, A., Paris, F., Elaouad-Debbaj, Z., 2004. Biostratigraphy, biodiversity and palaeoenvironments of the chitinozoans and associated palynomorphs from the Upper Ordovician of the Central Anti-Atlas, Morocco. Rev. Palaeobot. Palynol. 130, 17–40.

Brenchley, P.J., Romano, M., Young, T.P., Štorch, P., 1991. Hirnantian glaciomarine diamictites—evidence for the spread of glaciation and its effect on Upper Ordovician faunas. In: Barnes, C.R., Williams, S.H. (Eds.), Advances in Ordovician Geology. Geological Survey of Canada Paper 90–9, pp. 325–336.

Brenchley, P.J., Marshall, J.D., Carden, G.A.F., Robertson, D.B.R., Long, D.G.F., Meidla, T., Hints, L., Anderson, T.F., 1994. Bathymetric and isotopic evidence for a short-lived late Ordovician glaciation in a greenhouse period. Geology 22, 295–298.

Brenchley, P.J., Carden, G.A., Hints, L., Kaljo, D., Marshall, J.D., Martma, T., Meidla, T., Nolvak, J., 2003. High-resolution stable isotope stratigraphy of Upper Ordovician sequences: constraints on the timing of bioevents and environmental changes associated with mass extinction and glaciation. Geol. Soc. Am. Bull. 115, 89–104.

Carls, P., 1975. The Ordovician of the Eastern Iberian Chains near Fombuena and Luesma (Prov. Zaragoza, Spain). Neues Jahrbuch für Geologie und Paläontologie, 150. Abhandlungen, pp. 127–146.

Chen, X., Rong, J., Fan, J., Zhan, R., Mitchell, C.R., Harper, D.A.T., Melchin, M.J., Peng, P., Finney, S.C., Wang, X., 2006. The global boundary stratotype section and point (GSSP) for the base of the Hirnantian Stage (the uppermost of the Ordovician System). Episodes 29, 183–196.

Colmenar, J., Álvaro, J.J., 2014. Integrated brachiopod-based bioevents and sequence-stratigraphic framework for a Late Ordovician subpolar platform, eastern Anti-Atlas, Morocco. Geol. Mag. 152, 603–620, http://dx.doi.org/10.1017/S0016756814000533

Copper, P., Jin, J., Desrochers, A., 2013. The Ordovician–Silurian boundary (late Katian–Hirnantian) of western Anticosti Island, E Canada: revised stratigraphy and benthic faunal correlations. Stratigraphy 10, 213–227.

Copper, P., Jin, J., 2014. The revised Lower Silurian (Rhuddanian) Becscie Formation, Anticosti Island, eastern Canada records the tropical marine recovery from the end-Ordovician Mass Extinction. Newsletters Stratigr. 47, 61–83.

Delabroye, A., Vecoli, M., 2010. The end-Ordovician glaciation and the Hirnantian Stage: a global review and questions about Late Ordovician event stratigraphy. Earth Sci. Rev. 98, 269–282.

Desrochers, A., Farley, C., Achab, A., Asselin, E., Riva, J.F., 2010. A far-field record of the end-Ordovician glaciation: the Ellis Bay Formation, Anticosti island, eastern Canada. Palaeogeogr. Palaeoclimatol. Palaeoecol. 296, 248–263.

Finnegan, S., Helm, N.A., Peters, S.E., Fischer, W.F., 2012. Climate change and the selective signature of the Late Ordovician mass extinction. Proc. Natl. Acad. Sci. U.S.A. 109, 6829–6834.

Fan, J., Peng, P.A., Melchin, M.J., 2009. Carbon isotopes and event stratigraphy near the Ordovician–Silurian boundary, Yichang, South China. Palaeogeogr. Palaeoclimatol. Palaeoecol. 276, 160–169.

Fernández-Nieto, C., Torres-Ruiz, J., Subías Pérez, I., Fanlo González, I., González López, J.M., 2003. Genesis of Mg-Fe carbonates from the Sierra Menera magnesite-siderite deposits, Northeast Spain: evidence from fluid inclusions, trace elements, rare earth elements, and stable isotope data. Econ. Geol. 98, 1413–1426.

Finney, S.C., Berry, W.B.N., Cooper, J.D., Ripperdan, R.L., Sweet, W.C., Jacobson, S.R., Soufiane, A., Achab, A., Noble, P.J., 1999. Late Ordovician mass extinction: a new perspective from stratigraphic sections in central Nevada. Geology 27, 215–218.

Fortuin, A.R., 1984. Late Ordovician glaciomarine deposits (Orea Shale) in the Sierra de Albarracin, Spain. Palaeogeogr. Palaeoclimatol. Palaeoecol. 48, 245–261.

Ghienne, J.F., 2003. Late Ordovician sedimentary environments, glacial cycles, and post-glacial transgression in the Taoudeni Basin, West Africa. Palaeogeogr. Palaeoclimatol. Palaeoecol. 189, 117–145.

Ghienne, J.F., 2011. The Late Ordovician glacial record: state of the art. Cuadernos del Museo Geominero 14, 13–21.

Gil-Peña, I., Barnolas, A., Villas, E., Sanz-López, J., 2004. La cordillera Pirenaica. El Ordovícico Superior de la Zona Axial. In: Vera, J.A. (Ed.), Geología de España. IGME and SGE, Madrid, pp. 473–475.

Gutiérrez-Marco, J.C., Ghienne, J.F., Bernárdez, E., Hacar, M.P., 2010a. Did the Late Ordovician African ice sheet reach Europe? Geology 38, 279–282.

Gutiérrez-Marco, J.C., Štorch, P., 1998. Graptolite biostratigraphy of the Lower Silurian (Llandovery) shelf deposits of the Western Iberian Cordillera, Spain. Geol. Mag. 135, 71–92.

Gutiérrez-Marco, J.C., Robardet, M., Rábano, I., Sarmiento, G.N., San José Lancha, M.A., Herranz Araújo, P., Pieren Pidal, A.P., 2002. Ordovician. In: Gibbons, W., Moreno, M.T. (Eds.), The Geology of Spain. The Geological Society, London, pp. 31–50.

Gutiérrez-Marco, J.C., Ghienne, J.F., Bernárdez, E., Hacar, M.P., 2010b. Did the Late Ordovician African ice sheet reach Europe? Geology 38, 279–282.

Hafenrichter, M., 1979. Paläontologisch-Ökologische und Lithofazielle Untersuchungen des "Ashgill-Kalkes" (Jungordovizium) in Spanien, vol. 3. Arbeit Paläontologie Institute, Würzburg, pp. 1–139.

Hammann, W., 1992. The Ordovician trilobites from the Iberian Chains in the province of Aragón, NE—Spain. The trilobites of the Cystoid Limestone (Ashgill Series). Beringeria 6, 1–219.

Harper, D.A.T., Rasmussen, C.M., Liljeroth, M., Boldgett, R.B., Candela, Y., Jin, J., Percival, I., Rong, J.-Y., Villas, E., Zhan, R.-B., 2013. Biodiversity, biogeography and phylogeography of Ordovician rhynchonelliform brachiopods. In: Harper, D.A.T., Servais, T. (Eds.), Early Palaeozoic Biogeography and Palaeogeography, 38. Geological Society, London, Memoirs, pp. 127–144.

Herranz Araújo, P., Gutiérrez-Marco, J.C., Pieren Pidal, A.P., Robardet, M., San José Lancha, M.A., Rábano, I., Sarmiento, G.N., 2003. The Ordovician succession from the western Iberian Ranges (NE Spain): a review with new data. In: Albanesi,

G.L., Beresi, M.S., Peralta, S.H. (Eds.), Ordovician from the Andes. INSUGEO, Serie Correlación Geológica, vol. 17. INSUGEO, San Miguel de Tucumán (Argentina), pp. 417–424.
Jones, D.S., Fike, F.A., Finnegan, S., Fischer, W.W., Schrag, D.P., McCay, D., 2011. Terminal Ordovician carbon isotope stratigraphy and glacioeustatic sea-level change across Anticosti Island (Quebec, Canada). Geol. Soc. Am. Bull. 123, 1645–1664.
Kump, L.R., Arthur, M.A., Patzkowski, M.E., Gibbs, M.T., Pinkus, D.S., Sheehan, P.M., 1999. A weathering hypothesis for glaciation at high atmospheric $PCO_2$ during the Late Ordovician. Palaeogeogr. Palaeoclimatol. Palaeoecol. 152, 173–187.
LaPorte, D.F., Holmden, C., Patterson, W.P., Loxton, J.D., Melchin, M.J., Mitchell, C.E., Finney, S.C., Sheets, H.D., 2009. Local and global perspectives on carbon and nitrogen cycling during the Hirnantian glaciation. Palaeogeogr. Palaeoclimatol. Palaeoecol. 276, 182–195.
Larson, T.E., Heikoop, J.M., Perkins, G., Chipera, S.J., Hess, M.A., 2008. Pretreatment technique for siderite removal for organic carbon isotope and C:N ratio analysis in geological samples. Rapid Commun. Mass Spectrom. 22, 865–872.
Le Heron, D.P., Ghienne, J.F., El Houicka, M., Khoukhi, Y., Rubino, J.L., 2006. Maximum extent of ice sheets in Morocco during the Late Ordovician glaciation. Palaeogeogr. Palaeoclimatol. Palaeoecol. 245, 200–226.
Loi, A., Ghienne, J.F., Dabard, M.P., Paris, F., Botquelen, A., Christ, N., Elaouad-Debbaj, Z., Gorino, A., Vidal, M., Videt, B., Destombes, J., 2010. The Late Ordovician glacio-eustatic record from a high-latitude storm-dominated shelf succession: the Bou Ingarf section (Anti-Atlas, Southern Morocco). Palaeogeogr. Palaeoclimatol. Palaeoecol. 296, 332–358.
Marshall, J.D., Brenchley, P.J., Mason, P., Wolff, G.A., Astini, R.A., Hints, L., Meidla, T., 1997. Global carbon isotopic events associated with mass extinction and glaciation in the late Ordovician. Palaeogeogr. Palaeoclimatol. Palaeoecol. 132, 195–210.
Melchin, M.J., Holmden, C., 2006. Carbon isotope chemostratigraphy in Arctic Canada: sea-level forcing of carbonate platform weathering and implications for Hirnantian global correlation. Palaeogeogr. Palaeoclimatol. Palaeoecol. 234, 186–200.
Melchin, M.J., Holmden, C., Williams, S.H., 2003. Correlation of graptolite biozones, chitinozoan biozones, and carbon isotope curves through the Hirnantian. In: Albanesi, G.L., Beresi, M.S., Peralta, S.H. (Eds.), Ordovician from the Andes. INSUGEO, Serie Correlación Geológica, vol. 1. INSUGEO, San Miguel de Tucumán (Argentina), pp. 101–104.
Monod, O., Kozlu, H., Ghienne, J.F., Dean, W.T., Günay, Y., Le Herissé, A., Paris, F., Robardet, M., 2003. Late Ordovician glaciation in southern Turkey. Terra Nova 15, 249–257.
Owen, A.W., Harper, D.A.T., Rong, J.-Y., 1991. Hirnantian trilobites and brachiopods in pace and time. In: Barnes, C.R., Williams, S.H. (Eds.), Advances in Ordovician Geology. Geological Survey of Canada, St. John's, Newfoundland, pp. 179–190, Paper 90-9.
Sarmiento, G.N., 2002. Lower Palaeozoic of the Iberian Cordillera. In: García-López, S., Bastida, F. (Eds.), Palaeozoic conodonts from northern Spain, vol. 1. Cuadernos del Museo Geominero, Madrid, pp. 281–298.
Schwab, V., Spangenberg, J.E., Grimalt, J.O., 2005. Chemical and carbon isotopic evolution of hydrocarbons during prograde metamorphism from 100 °C to 550 °C: Case study in the Liassic black shale formation of Central Swiss Alps. Geochim. Cosmochim. Acta 69 (7), 1825–1840.
Schultz, L.G., 1964. Quantitative Interpretation of Mineralogical Composition from X-ray and Chemical Data for Pierre Shale. U.S. Geol. Prof. Paper 391–c, pp. 1–31.
Underwood, C.J., Crowley, S.F., Marshall, J.D., Brenchley, P.J., 1997. High-resolution carbon isotope stratigraphy of the basal Silurian stratotype (Dob's Linn, Scotland) and its global correlation. J. Geol. Soc. 154, 709–718.
Vennin, E., Álvaro, J.J., Villas, E., 1998. High-latitude pelmatozoan-bryozoan mud-mounds from the late Ordovician northern Gondwana platform. Geol. J. 33, 121–140.
Villas, E., 1985. Braquiópodos del Ordovícico Medio y Superior de las Cadenas Ibéricas Orientales. Memorias del Museo Paleontológico de la Universidad de Zaragoza 1, 1–223.
Villas, E., Lorenzo, S., Gutiérrez-Marco, J.C., 1999. First record of a Hirnantia Fauna from Spain and its contribution to the Late Ordovician palaeogeography of northern Gondwana. Trans. R. Soc. Edinburgh: Earth Sci. 89, 187–197.
Villas, E., Vennin, E., Álvaro, J.J., Hammann, W., Herrera, Z.A., Piovano, E., 2002. The Late Ordovician carbonate sedimentation as a triggering factor of the Hirnantian glaciation. Bulletin de la Société géologique de France 173, 569–578.
Villas, E., Vizcaïno, D., Álvaro, J.J., Destombes, J., Vennin, E., 2006. Biostratigraphic control of the latest-Ordovician glaciogenic unconformity in Alnif (Eastern Anti-Atlas, Morocco), based on brachiopods. Geobios 39, 727–737.
Villena, J., 1976. Estudio geológico de un sector de la Cordillera Ibérica comprendido entre Molina de Aragón y Monreal (provincias de Guadalajara y Teruel). Boletín Geológico y Minero 87, 329–335.
Vizcaïno, D., Villas, E., Herrera, Z., Álvaro, J.J., 2004. Informe preliminar sobre la presencia de trilobites hirnantienses (Ordovícico terminal) en la Pizarras de Orea de las Cadenas Hespéricas (NE de España). Geotemas 6, 315–317.
Wang, K., Chatterton, B.D.E., Wang, Y., 1997. An organic carbon isotope record of Late Ordovician to Early Silurian marine sedimentary rocks Yangtze Sea, South China. Palaeogeogr. Palaeoclimatol. Palaeoecol. 132, 147–158.
Webby, B.D., Droser, M.L., Paris, F., Percival, I. (Eds.), 2004. The Great Ordovician Biodiversification Event. Columbia University Press, New York, NY, p. 484p.